Pharmaceutical Research, Vol. 23, No. 6, June 2006 (© 2006)
DOI: 10.1007/s11095-006-0141-9

Research Paper

Glucose Partition Coefficient and Diffusivity in the Lower Skin Layers

Enam Khalil,[1,3] Kosmas Kretsos,[2] and Gerald B. Kasting[2]

Received October 16, 2005; accepted January 27, 2006

Purpose. This work aims to estimate the diffusivity and partitioning of glucose in the dermis and the viable epidermis of human skin.
Methods. The partition coefficient of glucose between phosphate-buffered saline and dermis, tape-stripped epidermis (TSE), stratum corneum (SC), and split-thickness skin, was measured *in vitro* using human cadaver skin. Glucose permeability across dermis and tape-stripped split-thickness skin (TSS) was measured using side-by-side diffusion cells. Glucose desorption from TSE and human epidermal membrane (HEM) was measured. All measurements were conducted at 32°C.
Results. The partition coefficient for glucose [mean ± SD (no. of samples)] was 0.65 ± 0.09 (n = 25) for dermis, 0.81 ± 0.06 (n = 10) for TSE, and 0.53 ± 0.12 (n = 9) for SC. Glucose diffusivity in dermis was calculated to be $2.64 \pm 0.42 \times 10^{-6}$ cm^2/s (n = 14). Glucose diffusivities in the viable epidermis estimated from TSS permeation, TSE desorption, and HEM desorption were $0.075 \pm 0.050 \times 10^{-6}$ cm^2/s (n = 5), $0.037 \pm 0.018 \times 10^{-6}$ cm^2/s (n = 4), and $1.0 \pm 0.6 \times 10^{-6}$ cm^2/s (n = 4), respectively.
Conclusion. The tissue/buffer partition coefficient of glucose in all skin layers was found to be less than unity, suggestive of excluded volumes in each layer. Glucose diffusivity in human dermis was found to be one third of its value in water, indicative of hindered diffusion related to the structural components of the tissue. A substantially lower value for glucose diffusivity in viable epidermis is suggested.

KEY WORDS: dermis; diffusivity; glucose; partitioning; viable epidermis.

INTRODUCTION

Development of painless methods of measuring blood analyte concentrations has become an area of increasing interest, especially for the measurement of glucose (1). These methods are classified either as minimally invasive or noninvasive compared to blood sampling (2). Transdermal extraction of analytes offers an attractive method of noninvasive diagnostics. In this method, a sample of interstitial fluid from the epidermis or the dermis is extracted transdermally and is subsequently analyzed (e.g., for glucose). However, the passive diffusion of analytes from dermal interstitium to the surface is limited by the barrier properties of stratum corneum (SC) (3).

Several physicochemical and physiological factors can influence the fraction of drug present in the dermal interstitium. Consequently, it is important to establish a correlation between the blood glucose level and the skin glucose level. Schragger (4) reported that for blood sugar at levels above 160 mg/dL, a correlation between skin and blood glucose levels was established when glucose oxidase-impregnated paper was applied to the stripped skin. He also reported that the free glucose found in punch biopsy specimens of full thickness skin was approximately two thirds of the blood sugar. Using the open-flow microperfusion method, Regittnig *et al.* (5) found that the fasting glucose level in the interstitial fluid of human adipose tissue was about 60% of the arterialized plasma levels. Using *in vitro* methods, Halprin *et al.* (6,7) found the glucose content of the epidermis to be between 38 and 52% of the medium concentration, whereas the dermis content was slightly higher. Based on the epidermal glucose level, these investigators suggested that glucose is not only restricted to the intercellular epidermal volume, but it also gained access to the available intracellular space by diffusion across the epidermal cell wall. Tuchin *et al.* (8) used an optical method for the measurement of the diffusivity of glucose in human dermis *in vivo* and compared it to that in water at the same temperature. They concluded that glucose diffusion in the human dermis was hindered possibly by the structural components of the dermis.

Quantitative interpretation of the above results is complicated by the fact that the transport parameters of glucose in the viable skin layers are not well known. Tuchin *et al.*'s result (8) does speak directly to dermal diffusivity, yet it is subject to uncertainties (e.g., osmotic and convective perturbations) related to the high glucose concentrations (20–40% w/w) employed. Diffusivity and partitioning in viable epidermis have, to our knowledge, not been measured. This is due primarily to the fact that viable epidermis is an exceedingly difficult tissue to isolate and study. In the present work, the partition coefficients of glucose between phosphate-buffered

[1] Faculty of Pharmacy, The University of Jordan, Amman 11942, Jordan.
[2] College of Pharmacy, The University of Cincinnati Medical Center, Cincinnati, Ohio 45267-0004, USA.
[3] To whom correspondence should be addressed. (e-mail: ekayoub@ju.edu.jo or enamkhalil@netscape.net)

saline (PBS) and dermis, tape-stripped epidermis (TSE), SC, and split-thickness skin were measured *in vitro* using human cadaver skin. Glucose permeabilities in the dermis and in tape-stripped split-thickness skin (TSS) were measured at low concentration (5.5 mM or 0.1% w/v), and diffusivities were calculated from these data combined with partition coefficient and thickness measurements. As an independent check on viable epidermis and dermis properties, desorption kinetics of glucose from TSE, human epidermal membrane (HEM), and dermis were measured, and diffusivity was estimated from the initial part of the desorption curves. A comparison between the methods for obtaining viable epidermis parameters is presented.

MATERIALS AND METHODS

Chemicals

D-[^{14}C (U)]-Glucose at 1 mCi/mL activity and a radiochemical purity >99% was purchased from American Radiolabeled Chemicals, Inc. (St. Louis, MO, USA) and used within 8 months of the assay date. Because the glucose tissue/buffer partition coefficients were all of order unity and the permeabilities were those in aqueous skin layers, low levels of impurities are not expected to substantially alter the results. Unlabeled D-glucose, Dulbecco's PBS, and trypsin (obtained from porcine pancreas) were purchased from Sigma (St. Louis, MO, USA). Sodium azide was obtained from Fisher (Fair Lawn, NJ, USA). Soluene®-350 and Ultima Gold™ scintillation cocktail were purchased from Perkin-Elmer (Boston, MA, USA).

Skin Preparation

Frozen, split-thickness human cadaver skin having a nominal thickness of 300 μm was obtained from US Tissue and Cell (Cincinnati, OH, USA). The samples were obtained from back, thigh, and abdomen areas. The tissue was bathed for 24 h in a broad-spectrum antibiotic solution, and then slowly frozen in a 10% glycerin solution to minimize cellular damage. The glycerin was washed from the tissue prior to the experiments. Dermis and HEM were obtained by heat separation of the epidermal layer from the dermis. The skin was immersed in a water bath at 60°C for 1 min, and then the epidermal layer was gently peeled away. SC was obtained by incubating the epidermal layer at 8°C in 0.01% trypsin solution for 12 h. The epidermal cells were then removed by gentle brushing. The SC samples were then washed with PBS solution and incubated in trypsin inhibitor for another 12 h. They were then dried and stored in a desiccator at 8°C to be used within 1 week. Stripping of split-thickness skin was carried out using Scotch® Magic Tape™, 3M (St. Paul, MN, USA). Samples (~6 cm^2) were stripped 20 times. Each strip was taken following application of an 1800-g weight for 10 s. The stripping tape was removed using two forceps, gently and unidirectionally, yielding TSS. These samples were used in the diffusion experiments without further treatment. The TSE studied in desorption and partition coefficient experiments was obtained by heat separation of TSS and was used immediately after preparation.

Partition Coefficient Determination

All partition coefficient experiments employed Dulbecco's PBS containing 0.02% sodium azide and 1 g/L cold glucose (PBS/SA/G) as the aqueous medium. A tissue sample with an approximate area of 6 cm^2 was loosely positioned between two metallic screens and then placed in a conical bottom, screw-cap, borosilicate glass vial containing 3 mL of PBS/SA/G and 0.1 μCi of ^{14}C-glucose. The metal screens were used to prevent the adherence of the skin to the glass vial or the Teflon-lined cap. They allowed the bathing solutions to freely contact both sides of the skin. The vials were incubated in an air thermostat maintained at 32°C for not less than 15 h. The equilibrium time was established on the basis of a pilot study in which the concentration was monitored over 50 h. At the end of the experiment, the tissue was removed from the buffer solution, blotted dry, weighed, and dissolved in Soluene. The buffer and the tissue solutions were analyzed for ^{14}C by liquid scintillation counting (LSC). The partition coefficient was then calculated by dividing the glucose concentration, expressed as μg/mL of the wet tissue, by the glucose concentration in the buffer, expressed as μg/ml. Tissue volume was calculated from its weight using the appropriate density for the different skin strata, as discussed later in this section.

Permeability Experiments

The permeability experiments were carried out using side-by-side diffusion cells (PermeGear, Inc., Bethlehem, PA, USA) having a 1.77-cm^2 cross-sectional area. The skin samples were mounted between the two halves of the diffusion cells, and each half was filled with 6 mL of PBS/SA/G solution. The temperature was kept at 32°C using an external circulating water bath, and both chambers were magnetically stirred at 600 rpm. After a 2-h equilibration, the donor compartment was spiked with 0.1 mL of a 10 μCi/mL solution of ^{14}C-glucose in PBS/SA/G. Samples (0.1 mL) from the donor side were collected at 0.5, 25, 40, 60, and 180 min and were not replaced. Samples (0.5 mL) from the receptor side were collected at 1, 2, 4, 7, 10, 15, 30, 45, 60, 90, 120, and 180 min and were replaced with 0.5 mL of PBS/SA/G. At the end of the experiment, the skin was blotted dry, weighed, and dissolved in Soluene. The radioactivity of the collected aqueous samples and the dissolved skin samples was measured by LSC.

Glucose Desorption from TSE and Dermis

Equilibrium glucose uptake was achieved as in the partition coefficient experiments. After attainment of equilibrium, the metallic screens carrying the epidermal samples were removed from the vials, gently blotted on filter paper, and immediately weighed. They were then placed in new borosilicate vials containing 3 mL of PBS/SA/G and reattached to the rotating incubator. Desorption kinetics were followed by sequentially repeating this step and placing the metallic screens carrying the epidermal samples in new vials containing fresh PBS/SA/G solutions. The exchanges were conducted at 0.1, 0.5, 1, 2, 4, 6, 10, 15, 25, 40 min and 1.0, 1.5, 2.0, 3.0, 9.0, 24, 48, and 72 h. The entire contents of each vial

were analyzed for the amount of desorbed radioactivity by LSC. At the end of the experiment, the TSE samples were removed from the screen, blotted dry, and weighed. They were then dissolved in Soluene and analyzed by LSC. A similar procedure was followed for the study of desorption kinetics from isolated dermis. In this case, the vial exchanges were conducted at 0.1, 0.5, 1, 2, 4, 10, 30 min and 1.0, 2.0, 4.0, 5.0, 20, 24, and 48 h.

Glucose Desorption from HEM

The HEM was heat-separated from the dermis as described above. HEM was weighed and then placed in a conical bottom, screw-cap, borosilicate glass vial containing 1 mL of PBS/SA/G and 10 μCi of ^{14}C-glucose. The vials were incubated in a shaking water bath maintained at 32°C for 20 h to establish equilibrium. The tissue was then carefully removed from the buffer solution, blotted dry, and mounted on a side-by-side diffusion cell with the SC side to the left and the viable epidermal side to the right. Both sides of the diffusion cell were filled with 6 mL of PBS/SA/G solution. Samples (1.0 mL) were taken from both sides simultaneously and replaced by PBS/SA/G solution. Samples were taken at 0.5, 1, 2, 5, 15, 30 min and 1, 2, 3, 4, 6, 23, and 25 h. At the end of the diffusion experiment, the HEM was cut into two parts—the inner diffusion circle and the edges. Each part was separately weighed and dissolved in Soluene. The radioactivity of all liquid and skin samples was measured by LSC. Skin drug content was used in the mass balance calculations.

Skin Thickness Calculation

The thickness of epidermal, dermal, and split-thickness skin samples was estimated from their mass and surface area. This was achieved using densities of 1.12 and 1.075 g/cm^3 for epidermis and dermis, respectively (9). The density of split-thickness skin was taken to be the average of these two values, or 1.09 g/cm^3. Surface areas were determined by tracing the outline of each sample on a uniform thickness paper, cutting and weighing the tracing and comparing the mass with a standard.

Statistical Analysis

The partition coefficient and skin thickness values were compared using one-way analysis of variance (ANOVA). Groups having significant differences by ANOVA ($p < 0.1$) were subjected to pairwise comparison tests (Holm–Sidak method) at a significance level of $p = 0.05$. All tests were conducted using Sigma Stat Version 3.10 (SPSS, Inc. Chicago, IL, USA).

Glucose Permeability and Diffusivity Estimate

Permeability of TSS, TSE, and isolated dermis subjected to the permeability studies was calculated from the steady-state flux J_{SS} of the radiolabel and its concentration difference across the tissue ΔC after accounting for aqueous boundary layers (10). Thus,

$$P_{obs} = J_{SS}/\Delta C \tag{1}$$

$$P_m = \left[\frac{1}{P_{obs}} - \frac{1}{P_{aq}}\right]^{-1} \tag{2}$$

$$P_{aq} = D_{aq}/h_{aq} \tag{3}$$

where P_{obs} is the observed permeability, P_{aq} is the combined permeability of the aqueous layers (one on each side of the tissue), and P_m is the actual permeability of the tissue with the subscript m describing TSS, TSE, or dermis depending on the respective experiment.

The combined thickness of the aqueous layers ($h_{aq} = 2 \times 50\ \mu m = 100\ \mu m$) appearing in Eq. (3) was drawn from a published experimental work (10) using diffusion cells of a similar design. Both systems employed star head magnets rotating at 600 rpm to stir the donor and receptor compartments. The value of the thickness reported in (10) corresponds to aqueous solutions at 37°C; however, the viscosity correction for a 32°C experiment is negligible. The aqueous diffusivity of glucose at 25°C is $D_{aq} = 6.76 \times 10^{-6}$ cm^2/s (11). This value was corrected to $D_{aq} = 8.06 \times 10^{-6}$ cm^2/s at 32°C according to the Stokes–Einstein equation (12). Inserting these values into Eq. (3) yields

$$P_{aq} = \frac{8.06 \times 10^{-6}\,\mathrm{cm^2/s}}{0.010\,\mathrm{cm}} = 8.06 \times 10^{-4}\,\mathrm{cm/s} = 2.9\,\mathrm{cm/h} \tag{4}$$

This value was used in conjunction with Eq. (2) to calculate the permeability of TSS, TSE, and dermis. The ratios of the resistance of the double aqueous diffusion layer to that of the dermis, TSS, and TSE were calculated to be 0.03, 0.008, and 0.01, respectively, indicating that aqueous boundary layers played only a minor role in these studies.

For dermis, the individual sample thickness h_{de} and permeability P_{de} were used to calculate the product $D_{de}K_{de}$ according to

$$D_{de}K_{de} = P_{de}h_{de} \tag{5}$$

This product is often termed the membrane permeability, in which case P_{de} is called the permeability coefficient; however, for simplicity of notation, we will refer to P_{de} as permeability. Dermal diffusivity was then calculated as

$$D_{de} = D_{de}K_{de}/\overline{K}_{de} \tag{6}$$

where $\overline{K}_{de}$ was the average dermis/water partition coefficient for the donor. This procedure was chosen because K_{de} and P_{de} determinations were made on different tissue samples. To estimate transport properties in viable epidermis, a two-layer model was applied to the permeation data obtained on TSS. Thus, epidermal permeabilities for individual samples P_{ed} were estimated as

$$P_{ed} = \left[\frac{1}{P_{TSS}} - \frac{1}{P_{de}}\right]^{-1} \tag{7}$$

where the values of P_{de} and P_{TSS} were obtained from the studies with dermis and TSS, respectively. Epidermal diffusivity D_{ed} was then calculated as

$$D_{ed} = P_{ed}\overline{h}_{ed}/\overline{K}_{ed} \tag{8}$$

where the value of $\overline{K}_{ed}$ was the average value obtained from the partition studies on TSE, and $\overline{h}_{ed}$ was the average value of the calculated epidermis thickness. Alternative estimations of D_{ed} and D_{de} were made from the desorption profiles of glucose from TSE, HEM, and isolated dermis, respectively. These desorption profiles were analyzed with a homogeneous slab approach, which yields, for a slab of thickness h and diffusivity D with boundaries maintained at zero concentration, the general relationship (13):

$$\frac{M_t}{M_\infty} = 1 - \frac{8}{\pi^2}\sum_{n=0}^{\infty}\frac{1}{(2n+1)^2}\exp\left[\frac{-D(2n+1)^2\pi^2 t}{h^2}\right]. \quad (9)$$

At short times t, corresponding to $Dt/h^2 \ll 1$, this equation may be written in either of the following forms (13,14):

$$\frac{M_t}{M_\infty} = 4\left(\frac{Dt}{\pi h^2}\right)^{1/2} \quad (10)$$

or

$$M_t = 2C_m\sqrt{Dt/\pi}A \quad (11)$$

In Eqs. (9)–(11), M_∞ is the amount of glucose initially in the slab (either TSE, HEM, or dermis), and M_t is the amount desorbed as a function of time. In Eq. (11), C_m represents glucose concentration in the slab, which was calculated as the product of the experimentally determined tissue/buffer partition coefficient of glucose and the final concentration of the sorption solution. A is the cross-sectional area of the tissue exposed to the desorbing solution. Equation (10) was used to describe the TSE and isolated dermis results, and Eq. (11) was employed for the HEM results. In applying Eq. (11) to HEM desorption, A was chosen to be the cross-sectional area of the diffusion cell; the value of M_t so calculated represents desorption from one side of the tissue only. The different forms were used because h and M_∞ could be accurately estimated for the TSE and dermis experiments, whereas C_m was more accurately estimated for the HEM experiments. It is worth noting that the seemingly erroneous assumption of tissue homogeneity for HEM is valid in the very short times considered. For this specific time frame, the two sides of HEM do not interact, i.e., each side behaves as if it were the boundary of a semi-infinite medium. Because the mass transfer resistance of the SC side is far greater than the respective viable epidermis resistance, the short-time desorption results can be attributed exclusively to the viable epidermis side.

RESULTS

Mass Balance Calculation

The total radioactivity of the collected samples, the residual liquid, and the dissolved skin samples was compared to the amount dosed. Recovery was in the range of 100 ± 10%. Following the diffusion experiment, the average residual disintegrations per minute (DPM) in dermis was found to be 1.5% of the initial dose, whereas the average residual DPM in TSS was 0.6% of dose, indicating lower uptake of the glucose by TSS compared to dermis. The residual radioactivity of the HEM was measured following the side-by-side desorption experiment. Less than 0.05% of the dose was found in the central disk, whereas 2.3% of the dose was found in the skin clamped in the ground glass joint. Thus, there was little evidence for binding of ^{14}C-glucose to the HEM, but some evidence for lateral diffusion of glucose within the tissue. Using the vial desorption method, the residual radioactivity of the TSE was found to be 0.2% of the dose.

Partition Coefficient Measurements

Table I lists the results of the partition coefficient and thickness measurements. Glucose tissue/buffer partition coefficients for different skin layers were significantly different by ANOVA ($p < 0.001$). Pairwise comparisons indicated significant differences between all pairs. Significant differences ($p = 0.024$) were found between K_{de}, K_{ed}, and K_{SC} values obtained from different donors. The calculated h_{de} values (510 ± 40 μm) were substantially higher than the nominal thickness of the split-thickness skin (300 μm). Furthermore, similarly higher than nominal thickness values [510 ± 30 μm ($n = 4$)] were found for TSS (donor no. 4 only—data not shown). The discrepancy between the nominal and calculated dermal thicknesses is likely to reflect the uncertainty of the dermatoming process combined with a small hydration effect because the weight of the dermis samples increased by an average of 7% during the experiments. There were no significant differences between donors for the h_{de} values, whereas the opposite was true for h_{ed}. A glucose partition coefficient was also measured using the

Table I. Tissue/Buffer Partition Coefficients (μg/mL Wet Tissue ÷ μg/mL Buffer) and Thickness for Human Skin Samples

	Dermis		TSE		SC
Donor no.	K_{de}	h_{de} (μm)	K_{ed}	h_{ed} (μm)	K_{SC}
1	0.52 ± 0.1 (6)	480 ± 60 (9)	0.87 ± 0.15 (3)	76 ± 15 (5)	0.49 (1)
2	0.68 ± 0.01 (3)	540 ± 150 (7)		40 ± 19 (3)	0.66 ± 0.13 (2)
4	0.62 ± 0.02 (8)	470 ± 80 (8)		26 ± 9 (2)	0.44 ± 0.12 (6)
5	0.78 ± 0.09 (4)	550 ± 80 (4)	0.75 ± 0.10 (3)	73 ± 4 (3)	
6	0.67 ± 0.10 (4)		0.82 ± 0.03 (4)		
Mean ± SD	0.65 ± 0.09	510 ± 40	0.81 ± 0.06	53 ± 24	0.53 ± 0.11

Values are expressed as mean ± SD (no. of samples).
TSE = tape-stripped epidermis; SC = stratum corneum.

Table II. Permeability and Diffusivity of Glucose in Lower Skin Layers (Mean ± SD)

Donor (no. of samples)	P (cm/h)	$DK \times 10^6$ (cm^2/s)	$D \times 10^6$ (cm^2/s)
Dermis			
1[a] (4)	0.110 ± 0.009	1.52 ± 0.29	2.96 ± 0.56
1[a] (4)	0.060 ± 0.014	1.11 ± 0.42	2.16 ± 0.81
4 (6)	0.10 ± 0.01	1.44 ± 0.19	2.80 ± 0.36
Mean ± SD	0.090 ± 0.026	1.36 ± 0.22	2.64 ± 0.42
CV (%)	29%	16%	16%
TSS			
4 (5)	0.020 ± 0.013	–	–
Epidermis[b]			
4 (5)	0.034 ± 0.024	0.057 ± 0.040	0.075 ± 0.050

[a] Same donor tested in different experiments.
[b] Calculated from Eqs. (7) and (8) as described in the text.

split-thickness skin for the purpose of skin characterization and found to be 0.69 ± 0.01 (n = 4). The value was intermediate between K_{de} (0.66 ± 0.09) and K_{ed} (0.81 ± 0.06) as expected.

Permeability Measurements

Table II summarizes the results of the glucose permeation studies in dermis and TSS, as well as calculations of epidermal permeability and diffusivity. Glucose diffusivity in dermis was found to be 2.64 ± 0.42 × 10^{-6} cm^2/s, about 33% of its value in water at 32°C. The estimated value for epidermal diffusivity was 0.075 ± 0.050 × 10^{-6} cm^2/s (n = 5), about 30-fold lower than that in dermis.

Desorption Measurements

Figure 1 shows the time course of glucose desorption from TSE using the vial immersion methodology. Although a substantial fraction of radiolabel was desorbed within the first minute (corresponding to 0.13 $h^{1/2}$), there was evidence for a slower process as well. We analyzed the data by considering that the first 30 s of desorption could be described as a square-root-of-time release process using Eq. (10). The diffusivities so calculated are shown in Table III, and the desorption profiles calculated from these values using Eq. (9) are shown in the figure. The average value of D_{ed} obtained from the analysis was 0.037 ± 0.019 × 10^{-6} cm^2/s, which is in the same range as the result reported for D_{ed} in Table II. Both of these values are much lower than the dermal diffusivity, but both are potentially influenced by residual SC on the tissue samples.

Table III. Diffusivity of Glucose in Viable Epidermis Calculated from the TSE Desorption Using Eq. (10)

Property	Units	Donor (sample) 4 (A)	4 (B)	2 (C)	2 (D)	Mean ± SD
M (30 s)	µg	12.0	18.8	5.7	6.9	10.9 ± 6.0
M_∞	µm	15.7	23.5	19.5	24.1	20.7 ± 3.9
h	µm	21	36	98	76	58 ± 35
$\sqrt{D} \times 10^3$	$(cm^2/s)^{1/2}$	0.13	0.23	0.23	0.18	0.19 ± 0.05
$D \times 10^6$	cm^2/s					0.037 ± 0.019

The data are shown in Fig. 1.

The HEM desorption method using side-by-side diffusion cells was devised to test whether another experimental approach could yield an epidermal glucose diffusivity with less chance of influence by the SC. Figure 2 presents glucose desorption from HEM (one side SC, the other viable epidermis) using this method. As in the TSE desorption studies, there was evidence for both rapid and slow desorption processes; in this case, the slow process may well be attributable to desorption from SC. However, the rapid phase for the viable epidermal side of the tissue was faster than that for TSE. Table IV summarizes the epidermal diffusivity calculations for this experiment based on applying Eq. (11) at a time of 30 s (0.13 $h^{1/2}$). The mean value of D_{ed} so calculated was 1.0 ± 0.6 × 10^{-6} cm^2/s, which is about 20-fold higher than

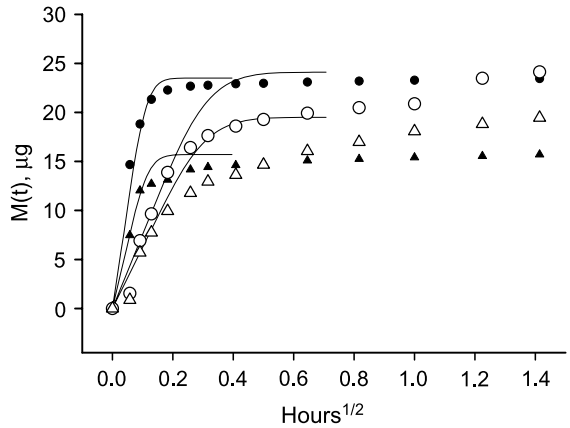

Fig. 1. Desorption of glucose from tape-stripped epidermis (TSE) measured using the vial desorption technique. The figure shows desorption kinetics from four individual TSE samples. The lines are plotted according to Eq. (9) using the parameter values in Table III. ▲ 4 (A); ● 4 (B); Δ 2 (C); ○ 2 (D).

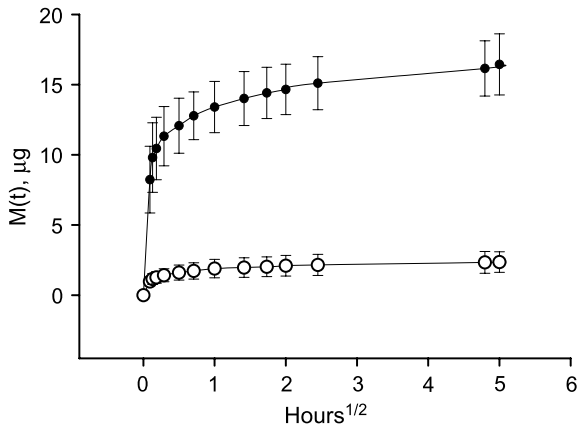

Fig. 2. Desorption of glucose from human epidermal membrane measured using the side-by-side diffusion cell. The figure shows desorption kinetics from the stratum corneum (open circles) and viable epidermis (closed circle) sides. Each point represents the mean ± SD of four samples.

Table IV. Diffusivity of Glucose in Viable Epidermis Calculated from the Human Epidermal Membrane Desorption Using Eq. (11)

Property		Donor (sample) 7 (A)	7 (B)	7 (C)	7 (D)	Mean ± SD
M (30 s)	μg	9.5	10.9	5.7	6.9	8.3 ± 2.4
C_m	μg/mL	756	748	751	771	757 ± 10
$\sqrt{D} \times 10^3$	$(cm^2/s)^{1/2}$	1.15	1.33	0.69	0.82	1.00 ± 0.29
$D \times 10^6$	cm^2/s					1.0 ± 0.6

The mean data are shown in Fig. 2.

the D_{ed} values obtained by other methods (Tables II and III) and only 3-fold lower than D_{de} (Table II). Possible reasons for these differences are discussed below.

The desorption method was also employed as a second independent method for the estimation of glucose diffusivity in the dermis. The desorption profiles so obtained (not pictured) were linear in the square root of time for times up to 4 min, consistent with Eq. (10). However, at longer times, they showed a slower approach to equilibrium than would be predicted from Eq. (9). Analysis of the data from 0 to 4 min according to Eq. (10) yielded an average dermal diffusivity of $5.6 \pm 1.5 \times 10^{-6}$ cm^2/s ($n = 4$).

DISCUSSION

Partition Coefficients

The experimental values of the partition coefficient obtained in this work were of the same order of magnitude values reported by Halprin and Ohkawara (7). Applying a different experimental and mathematical approach, Halprin *et al.* determined the tissue glucose content as a percent of the medium glucose concentration. They used pure human epidermis, tape-stripped epidermis, and epidermis contaminated with some dermis. Their results, based on skin dry weights, led to estimated values of K_{ed} ranging from 0.38 to 0.52. These values are slightly lower than the K_{ed} values obtained in this work, in which skin drug content was calculated based on the hydrated weight of the skin. Using full thickness human skin samples, Patel and Vasavada (15) measured the skin/buffer partition of isoproterenol HCl, a water-soluble drug, to be 0.546. This value supports our finding that the dermis/buffer partition coefficient of highly water-soluble compounds can be significantly less than unity.

Diffusivity of Glucose in the Dermis

Bashkatov *et al.* (16) used refractive index data to measure glucose diffusivity in human dura mater *in vitro* at 20°C. They postulated a structural similarity between the dura mater and human dermis. They extrapolated the dura mater diffusivity at 37°C to be 2.59×10^{-6} cm^2/s. Tuchin *et al.* (8) used the same technique to calculate glucose dermal diffusivity *in vivo* as $D_{de} = 2.56 \times 10^{-6}$ cm^2/s. The mean value obtained in the permeability study after extrapolation to 37°C (a 13% correction) was $D_{de} = 2.98 \times 10^{-6}$ cm^2/s. The extrapolation assumed that the temperature dependence of viscosity of the hydrated skin layers is similar to that of water. Glucose diffusivity in both dermis and dura mater was thus found to be approximately one third of that in water at the same temperature. According to Bashkatov *et al.* (16), two mechanisms may contribute to the restricted glucose diffusion through the interstitial matrix. The particles can stick to collagen fibrils, or they can be hindered by the size of the mesh spacing between the fibrils. Because glucose is a polar molecule, its diffusion can be hindered by the proteins, glycoproteins, and glycosaminoglycans (GAG) contained in the interstitial fluid. These molecules are excellent space filters, which provide selective barriers to the diffusion of small molecules. Thus, the penetration of glucose molecules into tissue is restricted. Ng *et al.* (17) used atomic force microscopy to directly image dense and sparse monolayers of bovine nasal cartilage aggrecan macromolecules. They were able to resolve both glycosylated and nonglycosylated regions of individual aggrecan monomers, as well as to achieve a nanometer-scale resolution of individual GAG chains. GAG–GAG spacing along the core protein was measured in the range of 3.2–4.4 nm. This value is only about ten times the radius of the glucose molecule (18); accordingly, hindered diffusion within the GAG–GAG space may be expected.

Analysis of the short-time dermal desorption data yielded a coefficient $D_{de} = 5.6 \times 10^{-6}$ cm^2/s, almost twice the value obtained in the permeability study. The discrepancy between the permeability and desorption results, combined with the observation that desorption equilibrium was only slowly achieved, reflects the sensitivity of the desorption technique to any heterogeneities existing in the tissue (19). Permeability experiments integrate diffusivity and partitioning across the tissue, whereas desorption results from an inhomogeneous sample may be asymmetrical (cf. Fig. 2). Thus, analysis of the dermal desorption data suggests that transport parameters for glucose vary across the tissue, possibly reflecting differences between the dense papillary dermis and the less dense reticular dermis. In the absence of a detailed study of such effects, it is wiser to rely on the permeability values (19).

Diffusivity of Glucose in the Viable Epidermis

In the presence of SC, the contribution of the viable epidermis to the diffusional resistance of the skin is often negligible, and the diffusivity of the viable epidermis has been considered to be similar to that of the dermis (20). In this work, the SC was stripped away to produce TSS, and the differences between dermis and TSS permeability were observed. Glucose permeability in TSS was found to be 22% of that in the dermis (Table II). By estimating epidermal properties according to the two-layer model, epidermal permeability and diffusivity were calculated as 38 and 3% of the dermal values, respectively (Table II). In obtaining glucose diffusivity using the two-layer model, the key is the efficiency of the tape-stripping procedure in removing the SC. The stripping protocol followed in this work seems sufficient to remove most of the SC from the cadaver skin based on published data. Pellett *et al.* (21) considered 15 tape strips enough to remove the SC from human skin obtained from abdomenoplasty after cosmetic surgery. Jarvis *et al.* (22) used the tape-stripping method to localize penetrants within human breast skin. The stripping was performed to the heat-separated

epidermis following the diffusion experiment. Fifteen tape strips were assumed to remove the SC. The content of the most hydrophobic drug in the SC strips compared to that remaining in the epidermis indicated the absence of corneocytes in the remaining epidermal layer. The efficiency of the stripping technique was discussed recently, and it was concluded that complete removal of the SC is practically not possible. Jacobi *et al.* (23) found that 66 ± 12% of the SC was removed with the first 20 tape strips from the human volunteers forearm, whereas Surber *et al.* (24) reported that complete removal of SC could be achieved after 100 stripping times. These findings might explain the low diffusivity value obtained in this work using TSS (Table II). Similarly, residual SC on one surface of TSE could retard desorption from the tissue and lead to an erroneously low value of D_{ed} in the vial desorption method (Fig. 1 and Table III). Using HEM mounted in side-by-side diffusion cells, a higher value of D_{ed} for glucose, equivalent to 30% of the dermal value, was obtained. This value can be considered with more confidence to represent the pure viable epidermis. The epidermal cellular structure might be responsible for the low diffusivity compared to dermis. According to the above argument, the three experimental approaches might be considered to estimate upper and lower limits for glucose diffusivity in the viable epidermis, with the true value most likely toward the upper end of this range.

CONCLUSION

The value of glucose diffusivity measured in human dermis by the *in vitro* permeability technique agreed well with values measured by others *in vivo*. The magnitude is about one third that of its diffusivity in bulk water. Tissue/buffer partition coefficients of glucose in both epidermis (TSE) and dermis were found to be less than unity. Permeation experiments in TSS and desorption experiments using TSE and HEM suggested that the diffusivity of glucose in epidermis is substantially lower than that in dermis, possibly because of the cellular structure.

NOTATION

HEM	Human epidermal membrane
LSC	Liquid scintillation counting
PBS/SA/G	Phosphate-buffered saline/sodium azide/glucose solution
SC	Stratum corneum
TSE	Tape-stripped epidermis
TSS	Tape-stripped split-thickness skin

Subscripts

aq	aqueous
de	dermis
ed	epidermis
m	general descriptor used in equations applicable to more than one kind of tissue sample, i.e., HEM and dermis
obs	observed
sc	stratum corneum
TSS	tape-stripped split-thickness skin

ACKNOWLEDGMENTS

This work was carried out during the sabbatical leave of Enam Khalil, which is financially supported by the University of Jordan, Amman, Jordan. Partial support was provided by NIOSH/CDC grant R01 OH07529. The authors acknowledge the assistance of Mr. Matthew Miller in conducting the experiments.

REFERENCES

1. S. Mitragotri, M. Coleman, J. Kost, and R. Langer. Analysis of ultrasonically extracted interstitial fluid as a predictor of blood glucose levels. *J. Appl. Physiol.* **89**:961–966 (2000).
2. D. J. Newman and A. P. F. Turner. Home blood glucose biosensors: a commercial perspective. *Biosens. Bioelectron.* **20**:2435–2453 (2005).
3. S. N. Murthy, Y.-L. Zhao, S. W. Hui, and A. Sen. Electroporation and transcutaneous extraction (ETE) for pharmacokinetic studies of drugs. *J. Control. Release* **105**:132–141 (2005).
4. A. H. Schragger. Ultramicro determination of epidermal glucose. *J. Invest. Dermatol.* **39**:417–418 (1962).
5. W. Regittnig, M. Ellmerer, G. Fauler, G. Sendlhofer, Z. Trajanoski, H.-J. Leis, L. Schaupp, P. Wach, and T. R. Pieber. Assessment of transcapillary glucose exchange in human skeletal muscle and adipose tissue. *Am. J. Physiol.: Endocrinol. Metab.* **285**:241–251 (2003).
6. M. K. Halprin, A. Ohkawara, and K. Adachi. Glucose entry into the human epidermis: I. The concentration of glucose in the human epidermis. *J. Invest. Dermatol.* **49**:559–560 (1967).
7. K. Halprin and A. Ohkawara. Glucose entry into human epidermis: II. The penetration of glucose into the human epidermis *in vitro*. *J. Invest. Dermatol.* **49**:561–568 (1967).
8. V. V. Tuchin, A. N. Bashkatov, É. A. Genina, Yu. P. Sinichkin, and N. A. Lakodina. *In vivo* investigation of the immersion-liquid-induced human skin clearing dynamics. *Tech. Phys. Lett.* **27**:489–490 (2001).
9. G. Altshuler, M. Smirnov, and I. Yaroslavsky. Lattice of optical islets: a novel treatment modality in photomedicine. *J. Phys., D. Appl. Phys.* **38**:2732–2747 (2005).
10. K. Tojo, J. A. Masl, and Y. W. Chien. Hydrodynamic characteristic of an *in vitro* drug permeation cell. *Ind. Eng. Chem. Fundam.* **24**:368–373 (1985).
11. L. G. Longsworth. Diffusion in the water–methanol system and the Walden product. *J. Phys. Chem.* **67**:689–693 (1963).
12. A. Martin, P. Bustamante, and A. H. C. Chun. *Physical Pharmacy*, Lea and Febiger, Malvern, 1993.
13. E. R. Cooper and B. Berner. Skin permeability. In D. Skerrow and C. J. Skerrow (eds.), *Methods in Skin Research*, John Wiley and Sons, New York, 1985, pp. 407–432.
14. J. Crank. *The Mathematics of Diffusion*, Clarendon Press, Oxford, 2001.
15. R. A. Patel and R. C. Vasavada. Transdermal delivery of isoproterenol HCl: an investigation of stability, solubility, partition coefficient, and vehicle effect. *Pharm. Res.* **5**:116–119 (1988).
16. A. N. Bashkatov, E. A. Genine, Y. P. Sinichkin, V. I. Kochubey, N. A. Lakodina, and V. V. Tuchin. Glucose and mannitol diffusion in human dura mater. *Biophys. J.* **85**:3310–3318 (2003).
17. L. Ng, A. J. Grodzinsky, P. Patwari, J. Sandy, A. Plaas, and C. Ortizd. Individual cartilage aggrecan macromolecules and their constituent glycosaminoglycans visualized via atomic force microscopy. *J. Struct. Biol.* **143**:242–257 (2003).
18. S. Mitragotri, M. E. Johnson, D. Blankschtein, and R. Langer. An analysis of the size selectivity of solute partitioning, diffusion, and permeation across lipid bilayers. *Biophys. J.* **77**:1268–1283 (1999).
19. G. B. Kasting, M. A. Miller, and P. S. Talreja. Evaluation of stratum corneum heterogeneity. In R. L. Bronaugh and H. I. Maibach (eds.), *Percutaneous Absorption*, Taylor & Francis, New York, 2005.
20. R. Scheuplein. Skin permeation. In A. Jarrett. *The Physiology and*

Pathophysiology of the Skin Academic Press, London, 1978, pp. 1693–1730.
21. M. A. Pellett, J. Hadgraft, and M. S. Roberts. The back diffusion of glucose across human skin *in vitro*. *Int. J. Pharm.* **193**:27–35 (1999).
22. C. A. Jarvis, C. M. Heard, and C. MCguigan. Targeted dermal delivery of highly potent anti-varicella zoster virus nucleoside analogues from saturated solutions and ethanolic oil-in-water creams. *J. Drug Target.* **11**:433–441 (2003).
23. U. Jacobi, H. J. Weigmann, J. Ulrich, W. Sterry, and J. Lademann. Estimation of the relative stratum corneum amount removed by tape stripping. *Skin Res. Technol.* **11**: 91–96 (2005).
24. C. Surber, F. P. Schwarb and E. W. Smith. Tape-stripping technique. In R. L. Bronaugh , and H. I. Maibach (eds.), *Percutaneous Absorption, Drugs–Cosmetics–Mechanisms–Methodology*, Taylor and Francis, Florida, 2005, pp. 399–410.